

FTIR-ATR Spectroscopic Technique on Human Single Intact Hair Fibre -A Case Study of Thyroid Patients

Sundaramoorthi Kamatchi ^{a*}, Sethu Gunasekaran ^b, Ethirajulu Sailatha^a, Raja Marthandam Pavithra^a, P. Kuppuraj^a
^a *Spectrophysics Research Laboratory, PG & Research Department of Physics, Pachaiyappa's college, Chennai - 600 030, Tamil Nadu, India.*

^b *Sophisticated Analytical Instrumentation Facility, St. Peter's Institute of Higher Education and Research, St. Peter's University, Avadi, Chennai - 600 054, Tamil Nadu, India.*

Abstract - Hypothyroid is one of the most common functional disorders of the thyroid gland. If there is not enough thyroid hormone in the blood stream, the body's metabolism slows down. One of the complications of hypothyroidism may include increase risk of heart disease, primarily due to increase levels of Low Density Lipoprotein (LDL), Protein and Glucose. Instead of analyzing blood to diagnose hypothyroid, hair could be used to detect hypothyroid by using Fourier Transform infrared – Attenuated Total Reflectance (FTIR-ATR) technique. Hair is made up of biomolecules such as alpha keratin, related proteins, lipids, glycogen and smaller amount of water. Hair can possibly be a biological sample that will reveal chemical deposition records in hair over extended periods of time, which may result in information of a diagnostics fingerprint in hair samples. The present study aims at employing FTIR-ATR spectroscopy for analyzing the hypothyroid hair fibre with elevated LDL, protein and glucose levels to detect spectral parameters, which might serve as biomarkers for identifying and detecting LDL, protein and glucose levels. The absorbance values at these specific modes of vibration varied significantly for hypothyroid from that of healthy subjects. The FTIR-ATR spectrum of human scalp hair fibre sample has been recorded in the mid-infrared region of 4000-450 cm^{-1} . The FTIR-ATR spectral analysis revealed the differences in some major metabolic components viz., (LDL), protein and glucose that clearly demarcated control and hypothyroid patient's hair scalp hair fibre. The method of internal ratio parameter is adopted in characterizing the hair sample quantitatively. Patients with hypothyroid showed increase in the peak height ratio of the I_{1450}/I_{1080} , I_{1180}/I_{1118} and I_{930}/I_{510} of lipids, proteins and glucose bands. These parameters could be used as a basis for deriving a spectral method for determine and measuring hypothyroid scalp hair. Fourth derivative spectroscopy reveals over 20 bands, providing more discrimination power to identify the differences and similarities between single hair fibre between control and hypothyroid. The study with FTIR-ATR technique proposed here is effective for screening of hypothyroid patients with higher lipids, proteins and glucose.

Keywords: Hypothyroid, Human hair fibre, Biomolecules, FTIR-ATR, Fourth derivative spectroscopy.

I. INTRODUCTION

Diagnosing disease through hair, in lieu of analyzing blood is quite challenging in the clinical laboratory. But the better utilization of science gives an opportunity to use hair as a tool in diagnosing diseases. Human hair is a complex tissue consisting of several morphological components [1]. Hair is an inert and chemically homogenous tissue [2]. Hair acts as a barrier to prevent water loss and to protect the scalp from sunlight and helping to maintain body heat. The barrier function of hair is mainly dependent on the cuticle and it is the outermost layer of the hair. Hair undergoes three phases during its growth cycle: the anagen, catagen and telogen phase. The anagen phase is active growing stage of the hairs. The catagen phase is the transitional stage between growing and dead. In the telogen phase, hair is in resting stage, when all growth has stopped and the dead hair begins to fall out [3]. The hair thread has a cylindrical structure, highly organized, formed by inert cells, most of them keratinized and distributed following a very precise and pre-defined design [4]. Hair is considered as a dead matter and it is only alive when it is inserted in the scalp. When the thread emerges, it becomes dead matter although it appears to be growing since the fibre follows increasing its length by a speed of about 1.0 cm/month [5-7].

However, as the human hair, on a simple level, is composed primarily of Biomolecules such as alpha keratin, related proteins, lipids, nucleic acids, glycogen (carbohydrates) and small amount of water [8]. Hair contains 65-95% of its weight in proteins, more 32% of water, lipid pigments and other components. Chemically about 80% of human hair is formed by a protein known as keratin with a high amount of sulphur coming from the amino acids cysteine, which may be re-oxidated under disulphidic bounding form. Cystine is very stable; this is the reason why human hair may be found relatively intact, even after several years after the death of an individual's [9, 10].

Keratin is one of the most abundant proteins, being the major component of hair, feathers, nails and horns of mammals. Keratin is high molecular weight polymer containing polypeptide chains formed by the condensation of L- amino acids. The bond that forms in upon condensation which links the amino acids called peptide bond [11]. Today, a growing number of proof-of-principle assays have been established using hair as a congenital hypothyroidism [12], Breast cancer [13], Rheumatoid arthritis [14] inflammation of the joints and surrounding tissues. Hair diagnostics would enable clinicians to monitor diseases frequently and easily and would have impact on the medical research and therapy. The biomolecules present

in the hair also make hair as a probe in the investigation of various disorders and diseases in human. Alike, hypothyroidism is one among the disorders that could be well identified using hair fibre.

Hypothyroid is one of the most common functional disorders of the thyroid gland, if there is not enough thyroid hormone in the blood stream, the body's metabolism slows down. One of the complications of hypothyroid may include increase risk of heart disease, primarily due to increase levels of LDL, Protein and Glucose among the people with under active thyroid [15]. The hair of hypothyroid affected people show high level of lipid and protein. As hair undergoes physical and biochemical changes due to hypothyroid, the spectra show variations that can be related to the hypothyroid condition in the subjects. The bio-molecular changes in the hair could be well scrutinized using molecular spectroscopy technique, one such is FTIR spectroscopic technique. Eventually, the deviation of control and hypothyroid disorder could be witnessed using FTIR-ATR spectroscopic technique.

II. MATERIALS AND METHODS

A. Sample Preparation and Handling

Samples of human scalp hair fibre (herein after referred as 'hair fibre') from 10 hypothyroid patients were obtained from a leading Hospital at Chennai, India, together with hair from 25 control persons. The single hair sample was plug from the hair root (i.e. anagen phase, active growing stage of the hair fibre) and kept separately in non-reactive plastic envelopes. Then, all of them were stored at room temperature until analysis. In order to eliminate any surface contaminations, specimens were washed by soaking in acetone for 1 minute followed by soaking in distilled water for the same time. Some of them were dirtier and are washed more and then the hair specimens are taken into laminar air flow to remove the water thoroughly.

All the hair samples were analyzed in the Mid IR region of $4000-450\text{ cm}^{-1}$. As water is a good absorbent of infrared radiation, it affects the actual spectral response of the test material and dominated in the FTIR spectrum of hair sample. After the removal of water, a root end of hair sample was placed on the IRE crystal. Force is applied by pressure gauge on the hair sample to prove good optical contact with the internal reflectance crystal. FTIR spectral measurements were carried at room temperature and each measurement was repeated to ensure the reproducibility of the spectra.

B. FTIR-ATR spectral Measurements

FTIR-ATR spectral measurements of human hair fibre samples were carried out at Sophisticated Analytical Instrumentation facility (SAIF-SPU), St. Peter's University, Avadi, and Chennai-600 054, using PerkinElmer Spectrum-Two FTIR Spectrophotometer with attenuated Total Reflectance accessory having highly reliable and single bounce diamond as its Internal Reflectance Element (IRE). The FTIR-ATR

spectroscopy is based on the phenomenon known as Total Internal Reflection (TIR) [16, 17]. This radiation strikes the interface between the IRE and the hair sample composed of a lower refractive index. This internal reflectance creates an evanescent wave that extends beyond the surface of the crystal into the hair sample held in contact with the crystal. It can be easier to think of this evanescent wave as a bubble of infrared that sits on the surface of the crystal. This evanescent wave protrudes only a few microns ($0.5\mu-5\mu$) beyond the crystal surface and into the sample. The depth of penetration of infrared radiation from denser IRE into the test material depends on refractive indices of the materials to be investigated and the wave number of the infrared radiation.

As the sample absorbs IR radiation at certain frequencies, the resultant totally reflected radiation (or) evanescent wave will be attenuated (altered) in regions of the infrared spectrum where the sample absorbs energy [16, 17]. This attenuated IR radiation of evanescent wave is passed back to the IR beam, which then exits the opposite end of the crystal and it is detected by the detector in IR spectrometer. The system generates an infrared spectrum.

The spectral recordings were done at 16 scans with resolution of 4 cm^{-1} . All the samples investigated were placed on the crystal of 2mm surface area with single bounce reflection has 350 cm^{-1} as its cutoff wave number; suitable pressure is given to the hair sample to make good optical contact between the sample and the IRE element (diamond). These spectra were subtracted against the background of air spectrum. After every scan, the crystal is cleaned with isopropyl alcohol or methanol soaked tissue and a background of new reference air was taken to ensure the crystal cleanliness. The fourth derivative spectrum is obtained with 149 smoothing point derivatization by Savitzky-Golay Method. The spectra were constructed using the software 'Spectrum', provided with FTIR Spectrum Two Spectrometer.

III. RESULTS AND DISCUSSION

The spectral analyses undertaken in this work primarily focus upon the qualitative and quantitative studies of hypothyroid and control hair fibre using ATR-FTIR spectroscopic technique. The FTIR absorption spectrum of human single intact hair fibre is represented in Fig.1 and the vibrational band assignments of biomolecules of human hair fibre is given in Table 1. In order to distinguish the spectral signatures of healthy and hypothyroid hair fibres in FTIR, the spectra obtained were overlaid and is represented in Fig.2. With respect to the internal ratio parameters, bar histograms (herein after referred as 'histogram') are constructed as shown in Fig.3. The fourth derivative spectra of hair fibre in the low frequency region between ($1800-450\text{ cm}^{-1}$) were studied, with an objective to discover the hidden FTIR spectral absorption. The fourth derivative spectra of each hypothyroid persons' with healthy were overlaid and compared in low frequency regions shown in Fig.4. The overlaid spectra of hair fibre, fourth derivative FTIR-ATR of each hypothyroid patient with control persons of each hypothyroid person with control subjects as shown in Fig.5. Fig.6 depicts the overlaid FTIR-ATR fourth derivative spectra of control and hypothyroid hair fibre in the regions (a) $1800-1300\text{ cm}^{-1}$ (b) $1200-900\text{ cm}^{-1}$ and (c) $600-450\text{ cm}^{-1}$.

A. FTIR Band Assignments of human hair fibre

The FTIR spectroscopy has been employed to monitor some specific molecules that also represent hypothyroid related signals such as proteins, lipids and glycogen. A band assignment is done with the idea of the group frequencies of the various analytes present in the sample. The prominent absorption peak 3280 cm^{-1} is due to the N-H stretching mode (Amide A) of protein [18]. The observed absorptions are the aliphatic C-H stretches of the saturated and unsaturated long chain fatty acids, alcohols and esters. The methyl (CH_3) asymmetric and symmetric modes were observed at 2955 cm^{-1} and 2930 cm^{-1} , respectively, and the methylene (CH_2) asymmetric and symmetric modes at 2875 and 2850 cm^{-1} [19]. In the IR spectra, very weak evidence of the protonated carboxyl group (COOH) exists, as reflected by the small band of the C=O stretching High Density Lipoprotein (HDL) at around 1745 cm^{-1} [20]. The broad and strong peak at 1645 cm^{-1} is due to C=O stretching coupled with an in- plane bending of the N-H and C-N stretching modes (Amide I band) [21]. While the amide II band centered at around 1540 cm^{-1} is due to C=O stretching coupled with C-N stretching and bending deformation of N-H in the protein backbones [22]. The absorptions in the keratin spectrum are attributed to the deformation and bending modes of the C-H/ CH_2 / CH_3 groups originating from the various amino acid (R) side chains [23]. The bands are exemplified as medium, broad absorption at 1450 cm^{-1} (LDL), while the band at 1340 cm^{-1} is due to bending deformation of CH_3 vibration of amino acid [24]. The absorption band at 1250 cm^{-1} is due to contributions of amide III and PO_2^- asymmetric stretching mode of nucleic acids [24]. The band observed at 1180 cm^{-1} is due to the C-OH groups of amino acid and the C-O groups of carbohydrate [22]. The spectral band at 1118 cm^{-1} is due to the glycogen [25]. The band around 1080 cm^{-1} is due to the contribution of symmetric stretching of PO_2^- of nucleic acid [26]. The subsequent strong and medium absorbance bands at 930 cm^{-1} can be associated with amide IV bands of the vibration $\text{O}=\text{C}-\text{N}$ [27]. The stretching vibrations of the S-S bonds of cysteine are visible in the $510\text{--}545\text{ cm}^{-1}$ region [27]. The noises observed in the spectra are due to the sampling of human single hair fibre.

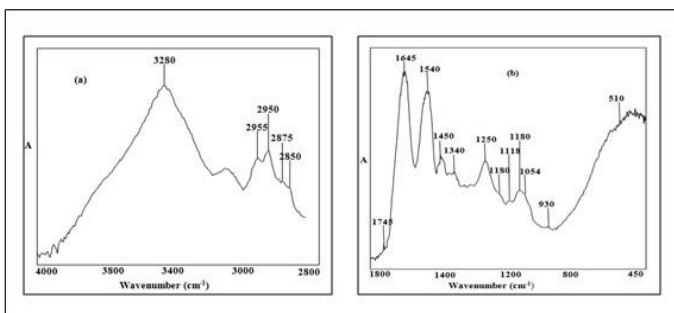


Fig. 1 FTIR-ATR spectrum of the human single intact hair fibre (a) High frequency region ($4000\text{--}2800\text{ cm}^{-1}$) and (b) low frequency region ($1800\text{--}450\text{ cm}^{-1}$).

Table 1 FTIR band assignments of human single hair fiber

S.No	Wavenumber (cm^{-1})	Vibrational Band Assignments
1	3280	ν N-H stretching
2	2955	ν_{as} CH_3 of proteins and lipids
3	2930	ν_{s} CH_3 of proteins and lipids
4	2875	ν_{as} CH_2 of proteins and lipids
5	2850	ν_{s} CH_2 of proteins and lipids
6	1745	C=O groups of cholesterol ester (HDL)
7	1645	Amide I band mainly due to C=O stretching vibrations amide groups
8	1540	Amide II band due to the δ N-H vibration strongly coupled to the ν C-N of protein
9	1450	δ C-H/ CH_2 / CH_3 of both lipid and protein groups (LDL)
10	1340	δ CH_3 of amino acid
11	1250	Amide III and ν_{as} PO_2^- stretching mode of nucleic acids
12	1180	C-OH groups of amino acid and the C-O groups of carbohydrate
13	1118	Stretching of Glycogen
14	1080	ν_{s} PO_2^- of nucleic acid
15	930	Amide IV vibration of $\delta\text{O}=\text{C}-\text{N}$
16	510	ν S-S of cysteine acid

ν -Stretching, ν_{as} -Stretching, δ - Bending/Deformation

The overlaid FTIR spectra of hypothyroid persons hair fibre along with control person given in Fig.2 emphasize the difference in the intensity of IR absorption exhibited by the hair fibres. Hence, no differences in the spectral signatures of the hair fibres were noticed. It is learnt that hypothyroid hair fibre doesn't bring any foreign functional groups; instead they are affecting the existing functional groups of biomolecules viz., proteins, lipids and glycogen. The variation in the optical density of each person is observed, due to the FTIR absorption of each hair fibre.

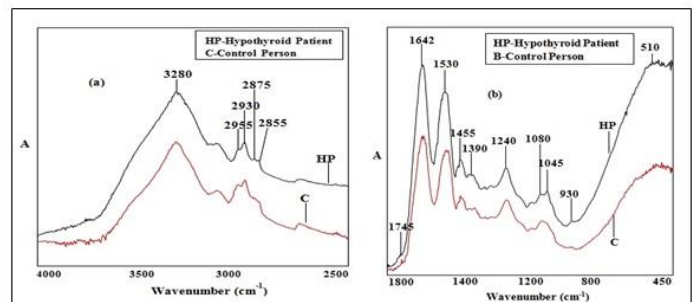


Fig. 2 Overlaid FTIR-ATR spectra of control and hypothyroid hair fibre (a) High Frequency region ($4000\text{--}2500\text{ cm}^{-1}$) and (b) Low Frequency region ($1800\text{--}450\text{ cm}^{-1}$).

In order to get exact deviations and the intensity of absorption in the discrimination of hypothyroid from control hair fibre, internal ratio parameters are calculated. This deals with the ratio of the intensity of Infrared absorption of specific Infrared bands. The Infrared bands are chosen with respect to its sensitivity Infrared. The sensitivity exhibited by the FTIR spectral bands of protein, lipids and glycogen bands due to the IR absorption of hypothyroid hair fibre clearly indicates that these are the key markers in the investigation of hypothyroid.

The sensitiveness witnessed in the IR absorption is due to the hike or reduction in the quantity of the sensible markers (functional groups) in the proteins, lipids and glycogen. Internal ratio parameter is calculated to fortify the results obtained from the FTIR intensity of absorptions. Internal ratio parameter ignores the difference in the amount of sample investigated, it nullifies the contradiction in the quantity of the samples and gives measured out exact deviations in the ratio of $R_1(I_{1450}/I_{1080})$, $R_2(I_{1180}/I_{1118})$ and $R_3(I_{930}/I_{510})$ of hypothyroid hair fibre.

The deviations in the internal ratio parameter of protein, lipid and glycogen of control and hypothyroid hair fibres are provided clearly in Table 2. The changes occur in the LDL and Nucleic acid bands of hair fibre show considerable changes in their intensity, but not in their respective position of the control and hypothyroid hair fibre. From the intensity ratio parameter (ie., $R_1(I_{1450}/I_{1080})$), absorption value is remarkably increased in the hypothyroid hair fibre from control one. The intensity ratio parameters $R_2(I_{1180}/I_{1118})$ and $R_3(I_{930}/I_{510})$ are calculated among the prominent absorption peaks due to the protein and glycogen. It is observed that the intensity values are increased in hypothyroid hair fibre from the control hair fibre. The small changes in the absorption is also appreciable in the FTIR-ATR spectra as it depends on the short existing, effective evanescent wave with $0.5\mu-5\mu$ depth of penetration. For better understanding in the deviation observed from internal ratio parameter calculations. The data obtained from internal ratio parameter is picturized using histograms as shown in Fig. 3. The differences in the height of the histogram are important in the discrimination of hypothyroid hair fibre from control subject. The histogram drawn between the ratios of LDL/Nucleic acid region in Fig.3 (a) shows the increase in the height of the histogram of hypothyroid. Fig.3 (b) and Fig.3 (c) alike the same is observed in the ratio of protein/glucose and Amide IV/Cysteine regions. The histograms support the results obtained from Internal Ratio Parameters.

Table 2 Internal Standard Ratio Parameters calculation of Lipid, protein and Glucose between control and hypothyroid scalp hair fiber.

Patient's	Control person's scalp hair fiber			Hypothyroid patient's scalp hair fiber		
	LDL 1450cm ⁻¹	Nucleic acid 1080cm ⁻¹	IRP Ratio I _{1450/1080}	LDL 1450cm ⁻¹	Nucleic acid 1080cm ⁻¹	IRP Ratio I _{1450/1080}
1	0.0149	0.0107	1.3925	0.0154	0.0136	1.4350
2	0.5600	0.0578	0.9688	0.0165	0.0159	1.0377
3	0.0163	0.0120	1.3583	0.0136	0.0090	1.5111
4	0.0560	0.0518	1.0810	0.0264	0.0207	1.2753
5	0.0264	0.0235	1.1330	0.0110	0.0089	1.2359
6	0.0260	0.0203	1.2807	0.0152	0.0115	1.3217
7	0.0161	0.0119	1.3529	0.0287	0.0212	1.3537
8	0.0130	0.0096	1.3541	0.0188	0.0137	1.3722
9	0.0175	0.0186	1.5000	0.0135	0.0083	1.6265
10	0.0308	0.0225	1.3811	0.0177	0.0126	1.4047
Patient's	Carbohydrate 1180cm ⁻¹	Glucose 1118cm ⁻¹	IRP Ratio I _{1180/1118}	Carbohydrate 1180cm ⁻¹	Glucose 1118cm ⁻¹	IRP Ratio I _{1180/1118}
	1	0.0488	0.0466	1.0475	0.0130	0.0138
2	0.0194	0.0181	1.0718	0.0154	0.0140	1.1000
3	0.0107	0.0097	1.1030	0.0088	0.0078	1.1282
4	0.0121	0.0107	1.1308	0.0240	0.0204	1.1764
5	0.0216	0.0211	1.0236	0.0087	0.0083	1.0481
6	0.0121	0.0111	1.0900	0.0133	0.0108	1.2314
7	0.0167	0.0153	1.0915	0.0119	0.0108	1.1018
8	0.0208	0.0196	1.0612	0.0126	0.0114	1.1044
9	0.0221	0.0208	1.0616	0.0083	0.0076	1.1184
10	0.0160	0.0146	1.0958	0.0128	0.0114	1.1228
Patient's	Amide IV 930cm ⁻¹	Cysteine 510cm ⁻¹	IRP Ratio I _{930/510}	Amide IV 930cm ⁻¹	Cysteine 510cm ⁻¹	IRP Ratio I _{930/510}
	1	0.0048	0.0215	0.2232	0.0103	0.0402
2	0.0356	0.1020	0.3490	0.0105	0.0288	0.3645
3	0.0072	0.0192	0.3750	0.0047	0.0066	0.7121
4	0.0079	0.0231	0.3419	0.0218	0.0142	1.5352
5	0.0066	0.0198	0.3333	0.0061	0.0130	0.4692
6	0.0130	0.0407	0.3194	0.0076	0.0230	0.3304
7	0.0060	0.0191	0.3141	0.0073	0.0187	0.3893
8	0.0107	0.0348	0.3074	0.0095	0.0244	0.3893
9	0.0145	0.0434	0.3341	0.0042	0.0056	0.7500
10	0.0058	0.0259	0.2259	0.0080	0.0259	0.3088

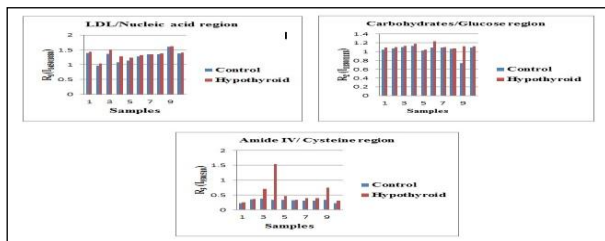


Fig. 3 Comparison of R_1 , R_2 and R_3 Intensity Ratio Parameters between Control and Hypothyroid scalp hair fiber.

However, although the quality of the spectra has been appreciably improved through the utilization of FTIR-ATR spectroscopy, the infrared spectrum of human hair keratin, lipids and glycogen, particularly within the wavenumber range of $1800-450\text{ cm}^{-1}$ is extremely complex. The spectral complexity is governed by the fact that there are number of absorption bands, especially in the proteins, lipids and glycogen region that are overlapped and provide no further qualitative information. This complication can be solved through the use of a mathematical manipulation method, by means of performing fourth derivative analysis on the FTIR-ATR spectra. The intensification of the fourth derivative analysis in this work is to study more deeply the underlying differences in the hair fibre between control and hypothyroid hair fibre. Hence, the 149 points smoothing model provides good resolution between component peaks and is selected as optimum condition for the analysis of hair fibre spectra.

The spectral difference between control and each hypothyroid fourth derivative spectra are illustrated in Fig.4. In general, it became apparent that the broad peaks that were present in the raw spectrum were resolved into a number of intense but sharp absorptions. The arrival of new bands at 1760 cm^{-1} , 1384 cm^{-1} , 1320 cm^{-1} and 575 cm^{-1} , 555 cm^{-1} , 548 cm^{-1} , 535 cm^{-1} , and 516 cm^{-1} shows that these are the exploration of unexplored biomarker in the hypothyroid with the raw spectra.

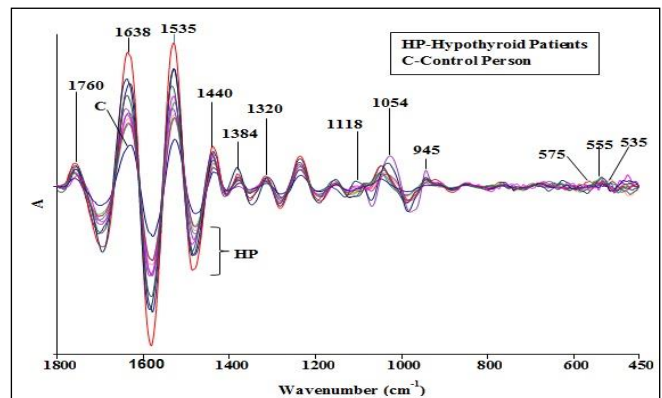


Fig.4 Fourth derivative spectra of each hypothyroid person with control subject at the region from $(1800-450\text{ cm}^{-1})$.

In the raw spectra failed to give the hidden spectral response of few functional groups of biomolecules in hair. Very weak evidence of the protonated carboxyl group (COOH) exists, as reflected by the small band of the C=O stretching at around 1745 cm^{-1} (HDL) in the raw spectra of hair. To disclose the hidden or weak infrared absorption characteristics of HDL, fourth derivative is employed. In the fourth derivative spectra, the carboxyl group (COOH) exists, demonstrating a sharp and strong band at around 1760 cm^{-1} due to the stretching (C=O) [28]. A band seen approximately at 1340 cm^{-1} is due to the δ (CH_2) deformation of amino acid in the raw spectra degenerates two bands observed at 1384 cm^{-1} and 1320 cm^{-1} are due to the deformation of C-H possessing different adjacent groups. The cysteine band originally at 510 cm^{-1} in the control raw spectrum of hair fibre, is separated into three distinguishable bands at

unequal intensity in the fourth derivative spectra. The weak absorption band at 575 cm^{-1} , 555 cm^{-1} , 548 cm^{-1} , 535 cm^{-1} and 516 cm^{-1} is associated to the vibrations of α - helix structure of cysteine.

The overlaid of each hypothyroid person with control subject was made and the fourth derivative FTIR-ATR spectra of hair fibre as shown in Fig. 5. From the fourth derivative spectra of control and hypothyroid hair samples, it is noticed that a band observed at 1054 cm^{-1} due to phosphate degenerates and exhibit a shoulder at 1087 cm^{-1} of C-O stretch of glucose, in the case of control hair. Whereas in the case of hypothyroid hair, the shoulder observed at 1087 cm^{-1} degenerates and clearly seen as a new band at 1118 cm^{-1} due to the increase in glucose by its C-O stretching vibration. So, a tiny band between glucose depicts the unregulated existence of hypothyroid.

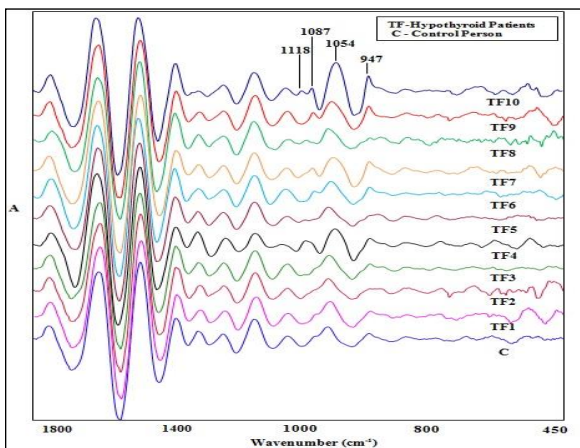


Fig.5 The overlaid spectra each hypothyroid person with control subject, fourth derivative FTIR-ATR spectra of hair fibre ($1800\text{--}450\text{ cm}^{-1}$).

The overlaid FTIR-ATR fourth derivative spectra of control and hypothyroid hair fibre in the regions (a) ($1800\text{--}1300\text{ cm}^{-1}$), (b) ($1200\text{--}900\text{ cm}^{-1}$) and (c) ($600\text{--}450\text{ cm}^{-1}$) are represented in Fig.6. From the FTIR derivative spectra, the spectral signatures are the same but the intensity of absorption varies from person to person in each hypothyroid hair fibre from control. Fig. 6 (a) depicts the absorption at 1758 cm^{-1} is related to C=O groups of cholesterol ester; an increase in its intensity is observed in hypothyroid hair fibre compared to the control one, as well as a red shift in the fourth derivative spectral region 1756 cm^{-1} is observed in the hypothyroid hair fibre. In the fourth derivative spectra, broad and strong absorption at 1045 cm^{-1} is due to $\nu_s\text{PO}_2^-$ of nucleic acid in the control and hypothyroid hair fibre. A red shift is observed in the hypothyroid and control hair fibre as shown in Fig.6 (b). Thus, what appeared to be a single absorption band is actually a number of bands of different secondary structural forms of the protein; the intensity of absorption of cysteine varies from person to person. Fig.6 (c) shows red shifts in the fourth derivative spectral regions of 575 cm^{-1} , 555 cm^{-1} , 549 cm^{-1} , 535 cm^{-1} and 516 cm^{-1} were observed in the healthy and hypothyroid hair fibre. These confirm the S-S stretching of cysteine vibration, which shifts due to the increase in the cysteine acid and its bonding with the adjacent groups.

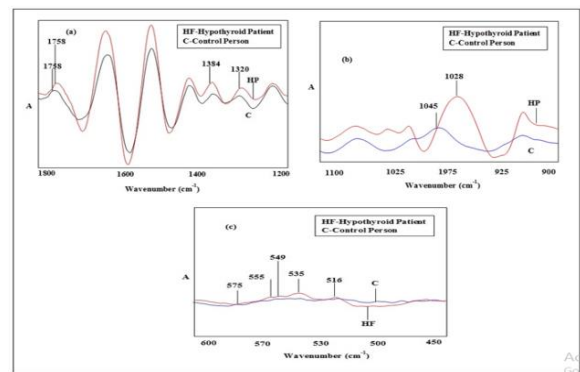


Fig.6 The overlaid FTIR-ATR fourth derivative spectra of control and hypothyroid hair fibre at the regions (a) $1800\text{--}1400\text{ cm}^{-1}$ (b) $1200\text{--}900\text{ cm}^{-1}$ (c) $800\text{--}450\text{ cm}^{-1}$

IV. CONCLUSION

The FTIR-ATR spectroscopic technique could be used as a powerful technique in the clinical laboratory to detect hypothyroid. FTIR-ATR spectroscopic technique exhibits qualitative information about biomolecules present and the method of internal ratio parameter is adopted in characterizing the hair sample quantitatively. Hair from subjects with hypothyroid showed an increase in the peak height ratios of the I_{1450}/I_{1080} , I_{1180}/I_{1118} , and I_{930}/I_{510} of lipids, proteins and glycogen bands. Fourth derivative spectroscopy revealed over 20 bands providing more discriminatory power to identify the differences and similarities between control and hypothyroid single hair fibre. This study demonstrates the potential for Attenuated Total Reflectance spectroscopy not only in the detection of hypothyroid, but in providing insight to the molecular and signaling processes involved in how hair acts as a biosensor in the detection of hypothyroid.

ACKNOWLEDGEMENT

The authors are thankful to the generous support (SAIF-SPU), St. Peter's University, Avadi and Chennai-600 054, for permitting to deploy the advanced instrumentation FTIR-ATR technique.

REFERENCES

- [1] C.R. Robbins, Chemical and Physical Behavior of Human Hair, Springer-Verlag Berlin Heidelberg, 2012, DOI 10.1007/978-3-642-25611-02.
- [2] A.B. El-Bialy, S.S. Hamed, S. Abd El-Mongy and E. Abd El Aziz. Mohamed, Concentration of some heavy metals in Egyptian human hair, International Journal of Basic and Applied Sciences, 3 (4) (2014) 414-419.
- [3] S. Kathyyn .Kalasinsky , Forensic analysis of hair by infrared spectroscopy 111-120.
- [4] Maria Valeria Robles velasco, Tania Cristina de as dias, Anderson Zanardi de Freitas, Nilson Dias Vieira Junior, Claudineia Aparecida sales de Oliveira Pinto, Telma Mary Kaneko, Andre Rolim Baby, Hair fibre characteristics and methods to evaluate hair physical and mechanical properties, Brazilian J. Pharmaceutical Sciences, 45 (2009) 1.
- [5] T. C. S. Dias analise da acaocodionadora de substancias cosmeticas adiciana dose malis antecapilar a base de tioglicolato de amonio. Sao Paulo, (2004) 106 [Dissertacao de Mestrado, Faculdade de Ciencias Farmaceuticas, Universidade de sao Paulo].
- [6] P. Cade, Chemical hair straighteners, waves and treatment products. Edison: Crode, (1995) 1-21.
- [7] V. M. Longo, V. F. Monteiro, A. S. Pinheiro, D. Terzi, J. S. Vasconcelos, c.A. Paskocimas, E.R. Leite, E. Longo, J. A. Varela, Charge density alterations human hair fibres: an investigation using electrostatic force microscopy, Int. J. Cosmet. Sci Oxford, 28 (2006) 95-101.

- [8] D. J. Lyman, J. M. Wijelath, Fourier transform infrared attenuated total reflection analysis of human hair: comparison of hair from breast cancer patients with hair from healthy subjects, *Appl. Spectros.*, 59 (2005) 26-32.
- [9] I. J. Kaplin, A. Schwan, H. Zahn, Effects of cosmetic treatments on the ultrastructure of hair, *cosmet. Toiletries Carol stream*, 97 (1982) 2-25.
- [10] R. C. C. Wagner, I. Joeekes, Hair protein removal by sodium dodecyl sulfate, *Colloids surf. B Biointerfaces Amsterdam*, 41 (2007) 7-14.
- [11] J.H. Bradbury, C.B. Anfinsen, F. M. Richards, In advances in protein chemistry, Academic press, U.S.A., 28 (1986) 111-211.
- [12] Lin S Y, Niu D M, Tu C P, et al, Diagnosis of congenital hypothyroidism from human anagen scalp hair infrared microscopy, *Ultrastruct. Pathol.*, 25 (2001) 357-360.
- [13] J. Donald, Lyman and Sheila G Fay, The effect of breast cancer on the Fourier Transform Infrared attenuated Total Reflection spectra of human hair, *ecancer medical science*, 8:405 (2015).
- [14] Hassan Imran Afridi, Tasneem Gul Kazi, Dermot Brabazon, Sumsun Naher, Association between essential trace and toxic elements in scalp hair samples of smokers rheumatoid arthritis subjects, *science of the total Environment*, 412-413 (2011) 91-100.
- [15] T. O' Brien, S. F. Dinneen, P. C. O' Brien, P. J. Palumbo, Hyperlipidemia in patients with primary and secondary hypothyroidism, *Mayo clin Proc.* 68 (1993) 860- [Pub Med].
- [16] C.F. Baulsir, R.J. Simler, *Advanced Drug Delivery Reviews*, 21 (1996) 191-203.
- [17] J.E. Katon, *Micron*, 27 (1996) 303-314.
- [18] G. Sankari, E. Krishnamoorthy, S. Jayakumaran, S. Gunasekaran, V. Vishnu Priya, Shyama, Subramanian, S. Subramanian, Surapaneni Krishna Mohan, Analysis of serum immunoglobulin's using Fourier transform infrared spectral measurements, *J. Biology and Medicine*, 2 (2010) 42-48.
- [19] W. Akhtar, H.G.M. Edwards, D.W. Farwell, M. Nutbrown, Fourier – Transform Raman spectroscopic study of human hair, *Spectrochimica Acta Part A*, 53 (1997) 1021-1031.
- [20] P. Barton, A Forensic Investigation of single human hair fibres using FTIR-ATR spectroscopy and Chemometrics, Honourthesis, Queensland University of Technology, 2011.
- [21] A.T. Tu, *Raman spectroscopy in Biology: Principles and applications*, John Wiley and Sons, 1982.
- [22] Y. J. Chen, Y. D. Cheng, H.Y. Liu, P. Y. Lin, C. S. Wang, Observation of biochemical imaging changes in human pancreatic cancer tissue using Fourier-transform infrared microspectroscopy, *Chang Gung. Med J*, 29(2006) 518-27.
- [23] P. Barton, A Forensic Taphonomy Investigation of single α – keratin fibres under Environmental stress using a Novel Application of FTIR-ATR Spectroscopy and chemometrics, Honours Thesis, Queensland University of Technology, 2004.
- [24] L. Bantignies, G. Fushs, G. L. Carr, G.P. Williams, D. Lutz, S. Marull, Organic reagent interaction with hair spatially characterized by infrared microspectroscopy using synchrotron radiation, *Int J Cosmet Sci*, 20 (1998) 381-94.
- [25] Xin Wang, Zeming Qi, Xingcun Liu, Shengyi Wang, Chengxizng Li, Gang Liu, Yin Xion, Tingting Li, jinqiu Tao, Yangcho Tian, The comparison of hair gastric cancer patients and from healthy persons studied by infrared microspectroscopy and imaging using synchrotron radiation, *cancer epidemiology* (2010), DOI: 10.1016.
- [26] M. J. Walsh, M.J. German, M. Singh, H. M. Pollock, A. Hammiche, M. Kyrgiou, IR microspectroscopy: potential applications in cervical cancer screening, *Cancer Lett*, 246 (2007) 1-11.
- [27] M. Gniadek, O.F. Nielsen, D. H. Christensen, H. C. Wulf, Structure of water proteins and lipids in intact human skin hair and nail, *J. Invest. Dermatol.*, 110 (1998) 393-398.
- [28] J.S. Church, A.L. Woodhead, *Biopolymers*, 42 (1997) 7-17.